NACA RM L52B26

NACA

RESEARCH MEMORANDUM

FLIGHT MEASUREMENTS OF THE EFFECTS OF SURFACE CONDITION ON THE SUPERSONIC DRAG OF FIN-STABILIZED PARABOLIC BODIES OF REVOLUTION

By H. Herbert Jackson

Langley Aeronautical Laboratory
Langley Field, Va.

NATIONAL ADVISORY COMMITTEE
FOR AERONAUTICS

WASHINGTON

May 2, 1952
Declassified November 2, 1954

1W

NACA RM L52B26

NATIONAL ADVISORY COMMITTEE FOR AERONAUTICS

RESEARCH MEMORANDUM

FLIGHT MEASUREMENTS OF THE EFFECTS OF SURFACE CONDITION ON THE SUPERSONIC DRAG OF FIN-STABILIZED PARABOLIC BODIES OF REVOLUTION

By H. Herbert Jackson

SUMMARY

Rocket-powered models have been flight tested at supersonic speeds to determine some effects of surface condition on the zero-lift drag of fin-stabilized parabolic bodies of revolution. Two configurations were utilized in the tests, a half-scale model of the NACA research model designated the RM-10 (fineness ratio 12.2) and a parabolic body of revolution having a fineness ratio of 8.91.

Three types of surface roughness were tested: (a) protuberances in the form of 60-mesh sand at saturation density, (b) depressions as found in an aluminum casting that has been partly ground but has not been machined completely smooth, the surface being pitted below the level at which grinding stopped, and (c) waviness. The Mach number range of the tests was approximately 0.8 to 2.2. The ranges of Reynolds number, based on body length, covered by the tests were from 15×10^6 to 75×10^6.

While the body covered with the 60-mesh sand showed a 20-percent increase in total drag over that of the smooth bodies, the other types of roughness tested showed no appreciable effect on total drag.

INTRODUCTION

As part of an NACA program of supersonic research, the Langley Pilotless Aircraft Research Division has made a series of flight tests at its Pilotless Aircraft Research Station, Wallops Island, Va., to investigate the effects of different types of surface roughness on the supersonic drag of fin-stabilized parabolic-arc bodies of revolution. It is of particular interest to determine the effects of different types and degrees of roughness because of the importance of surface drag to

the speed and range attainable by supersonic missiles. Also, it is important in connection with mass production of missiles to know what roughness can be tolerated without severe aerodynamic penalties.

Reported herein are zero-lift total-drag data for six models, four of a configuration having a fineness ratio of 12.2 (NACA RM-10) and two of another configuration having a fineness ratio of 8.91. Base-drag and side-pressure data were also obtained on two of the models of fineness ratio 12.2. Also included are drag data from references 1 and 2 on bodies of revolution which were of the same configuration as the bodies of fineness ratio 12.2 and 8.91, respectively, except that the model surfaces were smooth and fair.

The Mach number range of the data presented is from approximately 0.95 to 2.0 for the models of fineness ratio 12.2 and from 0.82 to 2.2 for the models of fineness ratio 8.91. The Reynolds number ranges were from 20×10^6 to 75×10^6 for the 12.2 fineness ratio and 15×10^6 to 63×10^6 for the 8.91 fineness ratio. These Reynolds numbers are based on body length.

SYMBOLS

C_{D_T}	total-drag coefficient based on maximum cross-sectional area of the body
C_{D_B}	base-drag coefficient based on maximum cross-sectional area of body $\left(\frac{p_b - p_o}{q_o}\right)\left(\frac{S_b}{S_f}\right)$
C_{p_s}	coefficient of side pressure related to free-stream conditions $\left(\frac{p_s - p_o}{q_o}\right)$
R	Reynolds number based on body length
M	Mach number
p_b	base pressure measured on annulus between rocket nozzle and model shell on bodies of fineness ratio 12.2
p_s	side pressure measured at $\frac{x}{l} = 0.9075$, 45° between fins on bodies of fineness ratio 12.2

p_o	free-stream static pressure
q_o	free-stream dynamic pressure
S_f	maximum cross-sectional area of body, 0.196 square foot for body of fineness ratio 12.2 and 0.307 square foot for body of fineness ratio 8.91.
S_b	base area of body, 0.0722 square foot for body of fineness ratio 12.2
x	axial distance from nose (station 0)
l	body length, 6.1 feet for body of fineness ratio 12.2 and 5.57 feet for body of fineness ratio 8.91
y	body radius

MODELS AND TESTS

The general arrangement of the test configurations and the body equations are given in figure 1. Photographs of the bodies of both fineness ratios 12.2 and 8.91 are shown in figure 2. Both configurations had parabolic-arc profiles, the body of fineness ratio 12.2 being described by one equation, whereas the body of fineness ratio 8.91 was described by two equations with vertexes located at the maximum body radius.

Three distinct types of roughness were tested: (a) protuberances in the form of 60-mesh sand, (b) depressions as found in partially ground cast aluminum, and (c) waviness. They were compared with bodies having smooth and fair surfaces.

All bodies of fineness ratio 12.2 except the wavy surface body were constructed of mahogany and cast magnesium alloy. The mahogany extended over the forward 84.6 percent of the body length. The model having the wavy surface was constructed of spun magnesium alloy with a tail section of cast magnesium alloy. The bodies of fineness ratio 8.91 were constructed entirely of mahogany except for dural tail fins.

The surface roughness, for those models on which it was possible, was measured by using a Brush surface analyzer with a stylus having a tip radius of 0.0005 inch. These measurements indicated that the reference 12.2 fineness ratio bodies (smooth, highly polished magnesium alloy) and the 8.91 and 12.2 fineness ratio Phenoplast mahogany surfaces had a maximum roughness (peak to valley) of 50 microinches (50×10^{-6} inches)

with an average value of approximately 25 microinches. The approximate root-mean-square value for this roughness is 8.2 microinches. This value was determined by using a method recommended by the manufacturer of the Brush surface analyzer. This degree of roughness is comparable with that of a polished fine-ground surface. Phenoplast, which is a phenolic-resin heat-resistant lacquer, was used on the test models because of its ability to withstand instantaneous heating in a bismuth-tin bath at 500° F without any noticeable change in surface condition. This 500° F is somewhat higher than the adiabatic wall temperatures attained by the test models in flight.

The 60-mesh sand was held to a mahogany surface by Phenoplast and covered the forward 84.6 percent of a 12.2 fineness ratio body at a saturation density (sand granule touching sand granule). The ratio of sand-grain diameter to total body length was about 13×10^{-4} (average grain diameter being 0.0098 inch). A photograph showing a magnified view of this type of surface is shown in figure 3(a).

The depressions were formed by spraying a 0.011- to 0.013-inch thickness of molten aluminum onto a mahogany surface. This application gave the surface a coarse sandpaper effect which was then sanded down so that only pits and flats remained, the surface between the depressions being smooth and free from waves. The depressions or pits varied in depth with a maximum depth of 0.0020 inch (as measured by a Brush surface analyzer) and covered approximately 40 percent of the sprayed aluminum surface. The average distance between the depressions was 1/32 of an inch. The average roughness of the over-all surface was about 0.0011 inch. Both the 12.2 and 8.91 fineness ratio bodies were tested with this type of roughness covering the forward 84.6 percent and 100 percent of the respective bodies. A photograph showing a magnified view of this type of surface is shown in figure 3(b).

The wavy surface was achieved by spinning longitudinal waves into a fineness ratio 12.2 spun magnesium alloy body which had a basic surface comparable to that of a smooth body. The waves covered the forward 84.6 percent of the body and had a peak-to-peak length of about 0.5 inch $\left(\text{wave-length-to-body-length ratio of about } 6.8 \times 10^{-3}\right)$ with a peak-to-valley depth of about 0.02 inch $\left(\text{wave-depth-to-body-length ratio of about } 2.7 \times 10^{-4}\right)$. A photograph of the model with this waviness can be seen in figure 3(c).

A two-stage propulsion system was employed for all models presented herein, with all models utilizing a 3.25 MK-7 aircraft rocket motor as the sustainer unit. Various booster rocket motors were utilized to obtain high Mach numbers. All models of fineness ratio 12.2 reported herein use NACA 5-inch rocket motors for boosters; whereas the reference

models were boosted as indicated in reference 1. The models of fineness ratio 8.91 were boosted by NACA 5-inch rocket motors and a 6.25-inch ABL Deacon rocket motor, whereas the model (reference 2) was boosted by a 5-inch HVAR motor. The booster units were all fin-stabilized and were attached to the sustainer motors by means of standard nozzle-plug type adapters. A photograph of a typical model-booster arrangement on the launching stand is shown in figure 4.

Data were reduced for the decelerating portion of the flight trajectory and atmospheric data were obtained from the SCR 584 tracking radar (modified by NACA) and by radiosonde observations. Velocity and total drag were obtained from the CW Doppler radar as described in reference 3. Also base drag and side pressure were reduced for the 12.2 fineness ratio models from data telemetered to a ground receiving station by instrumentation incorporating two pressure cells.

Base pressure for the models of fineness ratio 12.2 was measured inside the afterbody between the rocket nozzle and the skin by an open-ended tube located as shown in figure 5. The annular area around the rocket motor at the base was sealed from the forward part of the body to prevent internal air flow. The base-drag coefficient was computed with the assumption that the measured base pressure acts over the entire area of the base. The side pressure was measured by an orifice located on the smooth surface of the tail casting, 45° between the fins and at the 90.75-percent body-length station.

The flight tests of the models covered a range of Reynolds numbers (based on body length) from 15×10^6 to 75×10^6. In figure 6 the Reynolds number encountered in flight is plotted against Mach number.

The errors in the Mach number, pressure, and drag coefficient data for each individual model are probably within the values listed below:

M	Error			
	M	C_{D_T}	C_{D_B}	C_{p_s}
1.8	±0.005	±0.003	±0.002	±0.008
1.4	±0.005	±0.005	±0.003	±0.010
1.1	±0.005	±0.007	±0.005	±0.020
1.0	±0.005	±0.010	±0.010	±0.040

The body coordinates of the test models were all within 0.020 of the design values and all surfaces except those with stated roughnesses were smooth and fair. All bodies on which it was possible were highly polished at the time of launching.

RESULTS AND DISCUSSION

Drag results for the models of fineness ratio 12.2 are presented in figure 7. Both total-drag coefficient C_{D_T} and base-drag coefficient C_{D_B} are shown.

Compared in figure 7 with the mean-drag coefficient of five highly polished metal bodies (reference 1) are: (a) the drag of a model having roughness protruding from the surface in the form of 60-mesh sand at saturation density, (b) the drag of a model made to simulate a partly ground aluminum casting of which the surface was 60 percent smooth, the remainder being pitted approximately 0.002 inch below the level at which grinding stopped, (c) the drag of a highly polished smooth Phenoplast finished model, and (d) the drag of a model having longitudinal waves (0.02 inch deep and 0.5 inch long). It will be noted from the figure that neither the Phenoplast finish, the pitted surface, nor the wavy surface had any appreciable effect on the total-drag coefficient. The sandcoated surface, however, increased the total-drag coefficient substantially, in this case by approximately 20 percent. Also presented in figure 7 are the base-drag coefficients for the sandcoated model and the wavy-surface model compared with the mean-base-drag coefficient of smooth polished models (reference 1). These data indicate that the drag increase of the sandcoated model was not due to a change in base drag. The increase in total-drag coefficient is in all probability due to an increase of approximately 90 percent in viscous drag coefficient which has been found by drag component breakdown to be about 0.065 for the smooth bodies at $M = 1.4$. This 90-percent increase, of course, is obtained by considering the unknown amount of pressure drag on the sand particles to be viscous drag. Original estimates of the viscous drag coefficient by the methods outlined in references 4, 5, and 6 indicated an increase of 0.062 (approximately 100-percent increase) at Mach number 1.6 due to applying 60-mesh sand at saturation density.

Figure 8, which shows the variation of side-pressure coefficient C_{p_s} with Mach number for the sandcoated-surface and the wavy-surface models, as measured at $\frac{x}{l} = 0.9075$ and 45° between fins, indicates that the sandcoated surface had a less positive side pressure at the lower Mach numbers than the wavy surface. Although this difference at the lower Mach number is largely within the added accuracies, there may have been some effect due to a difference in boundary-layer thickness. The peaks shown in the side-pressure coefficient near Mach number 1.0 are probably caused by a shock moving downstream and over the side orifice as supersonic speeds are attained. Compared with the present

test data are values as interpolated from unpublished smooth full-scale RM-10 data, where the pressures were measured 45° between the fins and at the 89.42- and 95.22-percent stations. As can be seen, the pressure coefficients for the sand and wavy surfaces have the same trend as the smooth body with any effect due to the different surfaces diminishing rapidly with increasing Mach number.

Compared in figure 9 with total-drag coefficient of a model of fineness ratio 8.91 (model 2, reference 2) that was finished with clear lacquer to form a smooth and fair surface are: (a) the drag of a model made to simulate a partly ground aluminum casting (the entire body surface finished similarly to the body of fineness ratio 12.2 having the same surface) and (b) the drag of a smooth highly polished Phenoplast surface. The figure agrees with results from the body of fineness ratio 12.2 in that some degree of roughness due to pitting can be tolerated without being detrimental to the over-all drag. It will also be noted from figure 9 that not only are the drags of the Phenoplast finished model and the pitted surface of the simulated casting the same as that of the reference model over the supersonic range but also are the same over the transonic and subsonic range.

CONCLUSIONS

Free-flight tests have been conducted on bodies of parabolic profile having various types of surface roughness. Two configurations were tested, one having a fineness ratio of 12.2 and another a fineness ratio of 8.91. The test Reynolds numbers varied from 15×10^6 to 75×10^6. Within the limits of the investigation, the results indicated the following:

1. At very high Reynolds numbers at which the boundary layers are naturally turbulent, some degree of roughness due to pitting or waviness can be tolerated on a supersonic missile without an appreciable effect on total drag.

2. Roughness projecting from the surface of a supersonic missile at high Reynolds numbers can cause substantial drag increases. Sand (60-mesh) covering the forward 84.6 percent of an RM-10 test vehicle at saturation density increased the supersonic total-drag coefficient by about 20 percent (90 percent estimated increase in viscous drag) over that of a body having a smooth surface.

3. The base drag measured on the wavy body and on the sand-covered body was not markedly different from that of the smooth RM-10 research vehicles.

Langley Aeronautical Laboratory
National Advisory Committee for Aeronautics
Langley Field, Va.

REFERENCES

1. Jackson, H. Herbert, Rumsey, Charles B., and Chauvin, Leo T.: Flight Measurements of Drag and Base Pressure of a Fin-Stabilized Parabolic Body of Revolution (NACA RM-10) at Different Reynolds Numbers and at Mach Numbers from 0.9 to 3.3. NACA RM L50G24, 1950.

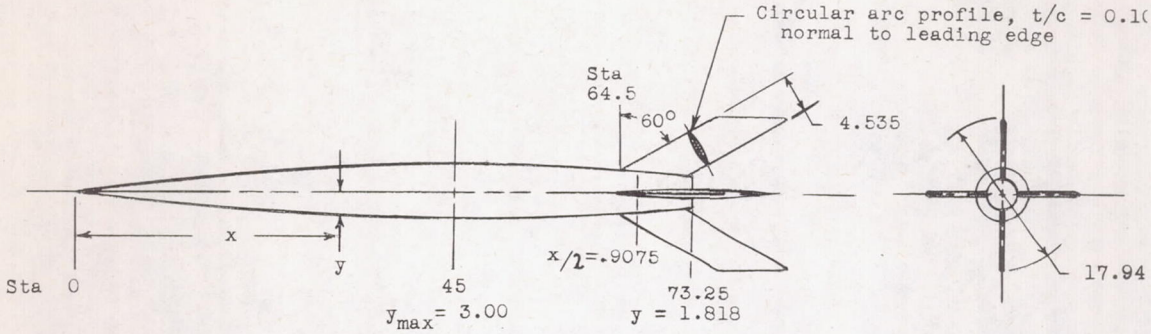
2. Katz, Ellis R., and Stoney, William E., Jr.: Base Pressures Measured on Several Parabolic-Arc Bodies of Revolution in Free Flight at Mach Numbers from 0.8 to 1.4 and at Large Reynolds Numbers. NACA RM L51F29, 1951.

3. Morrow, John D., and Katz, Ellis: Flight Investigation at Mach Numbers from 0.6 to 1.7 to Determine Drag and Base Pressures on a Blunt-Trailing-Edge Airfoil and Drag of Diamond and Circular-Arc Airfoils at Zero Lift. NACA RM L50E19a, 1950.

4. Hall, Charles F., and Fitzgerald, Fred F.: An Approximate Method for Calculating the Effect of Surface Roughness on the Drag of an Airplane. NACA RM A7B24, 1947.

5. Theodorsen, Theodore, and Regier, Arthur: Experiments on Drag of Revolving Disks, Cylinders, and Streamline Rods at High Speeds. NACA Rep. 793, 1944. (Supersedes NACA ACR L4F16.)

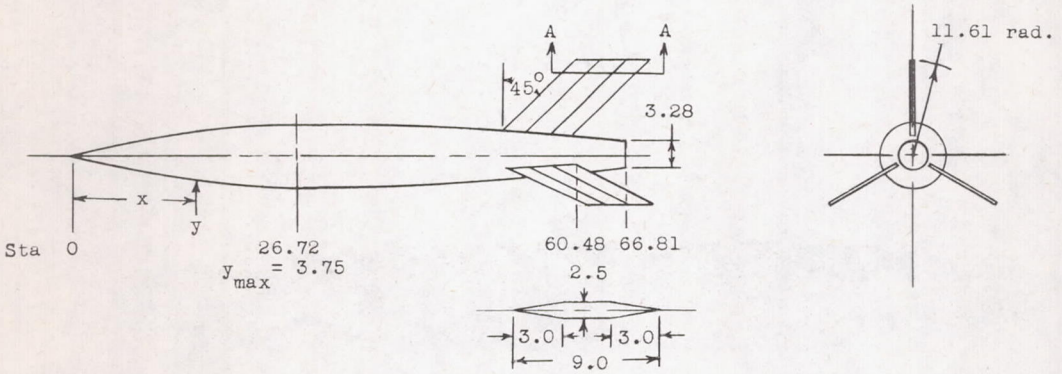
6. Schlichting, H.: Experimental Investigation of the Problem of Surface Roughness. NACA TM 823, 1937.



Half scale RM-10, body profile equation:

$$y = 3.00 - 0.0014814 (45 - x)^2$$

(a) Body of fineness ratio 12.2.



Section A-A
(Not to scale)

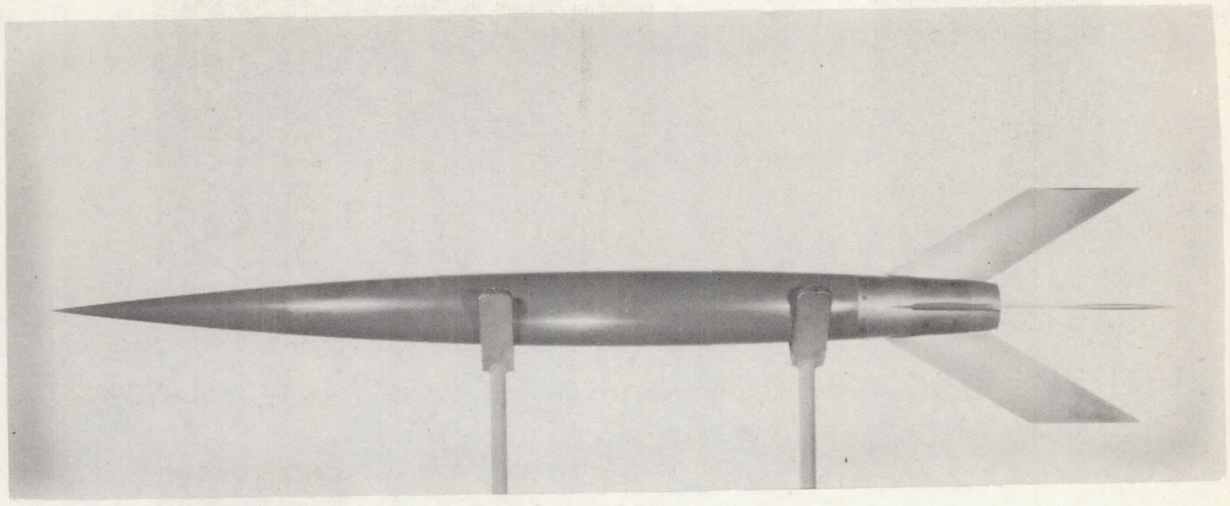
Body profile equation:

$0 < x < 26.72$ $\quad y = 3.75 - 0.005251 (26.72 - x)^2$

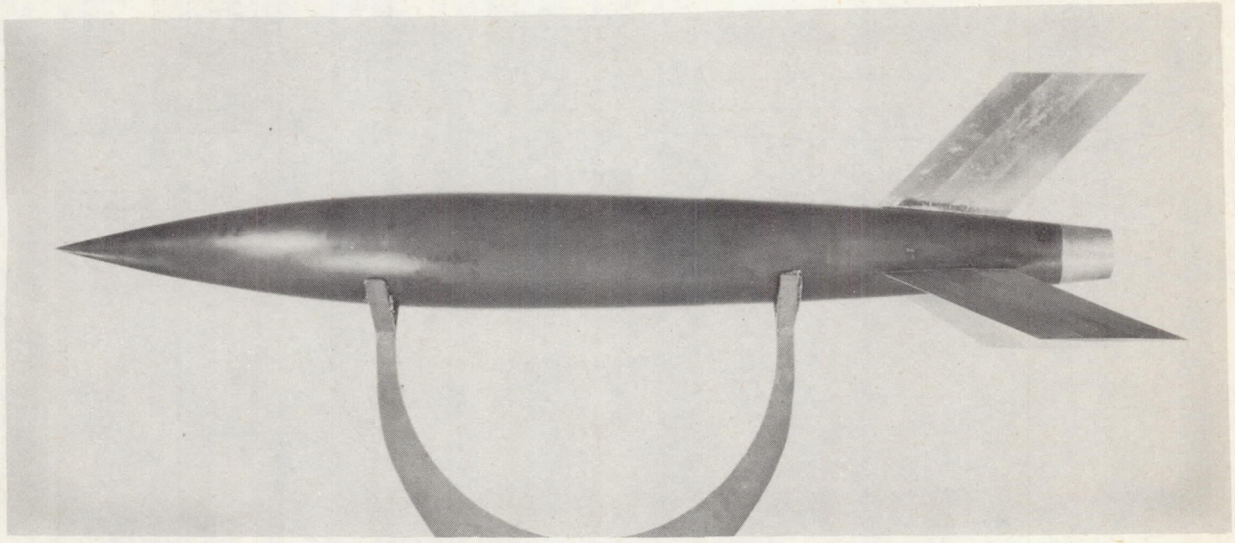
$26.72 < x < 66.81$ $\quad y = 3.75 - 0.001313 (26.72 - x)^2$

(b) Body of fineness ratio 8.91.

Figure 1.- General configurations of test models. (Dimensions are in inches.)

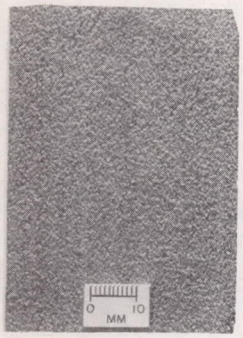


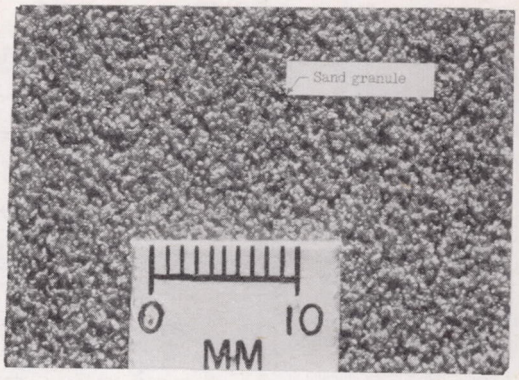
(a) Model of fineness ratio 12.2 (smooth Phenoplast surface). L-67884



(b) Model of fineness ratio 8.91 (smooth Phenoplast surface). L-71983

Figure 2.- General views of test models.

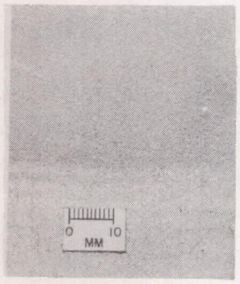


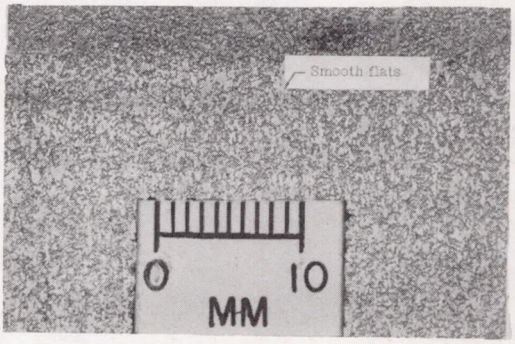


NACA Magnification 1X L-72990

Magnification 3X NACA L-72992

(a) Surface coated with 60-mesh sand.

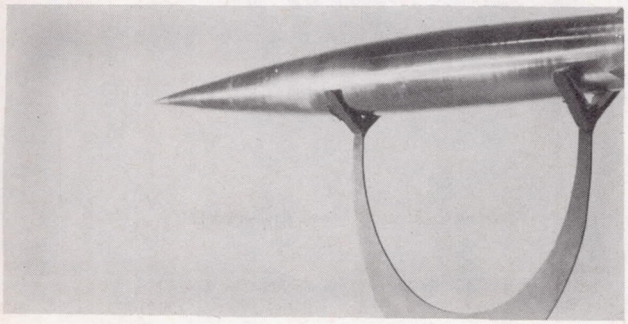




NACA Magnification 1X L-72991

Magnification 3X NACA L-72993

(b) Simulated cast aluminum surface.



NACA L-69687

(c) Wavy surface (oblique lighting to show waves).

Figure 3.- Photographs showing the various types of roughness utilized in tests.



Figure 4.- Typical model-booster arrangement on launching stand. Model of fineness ratio 8.91 with Deacon booster.

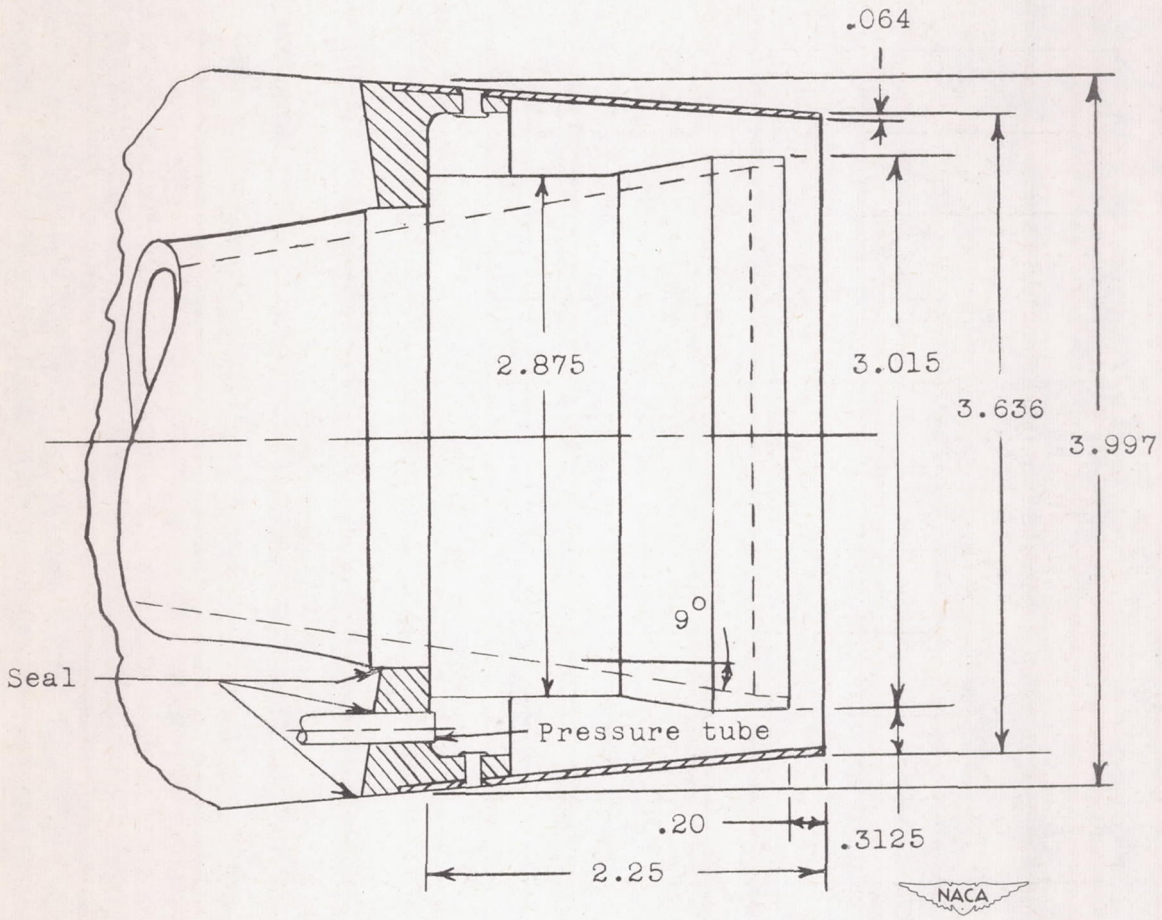


Figure 5.- Base-pressure-tube location for the models of fineness ratio 12.2. (Dimensions are in inches.)

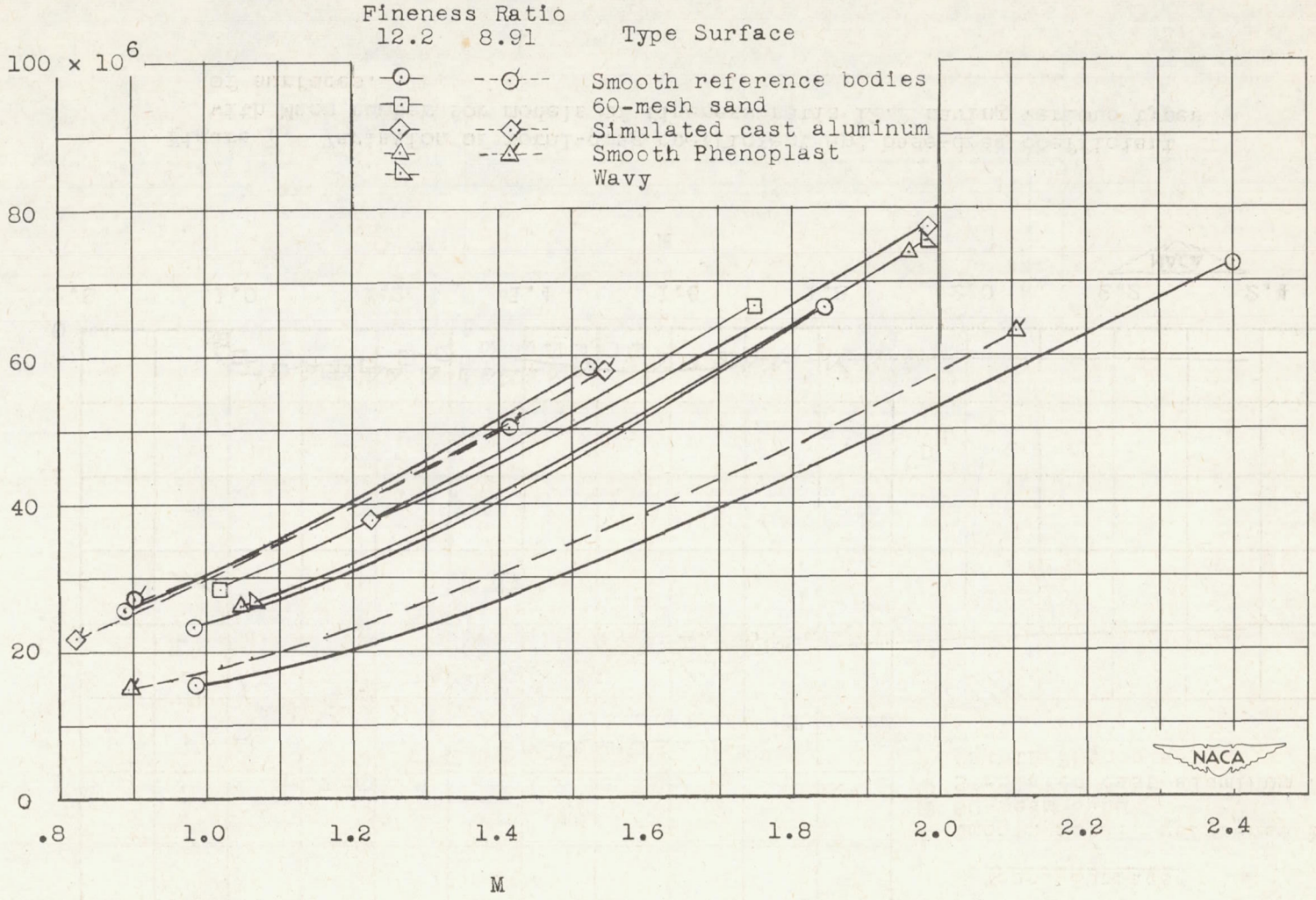


Figure 6.- Variation of Reynolds number with Mach number for the test and reference models. Reynolds number based on total body length.

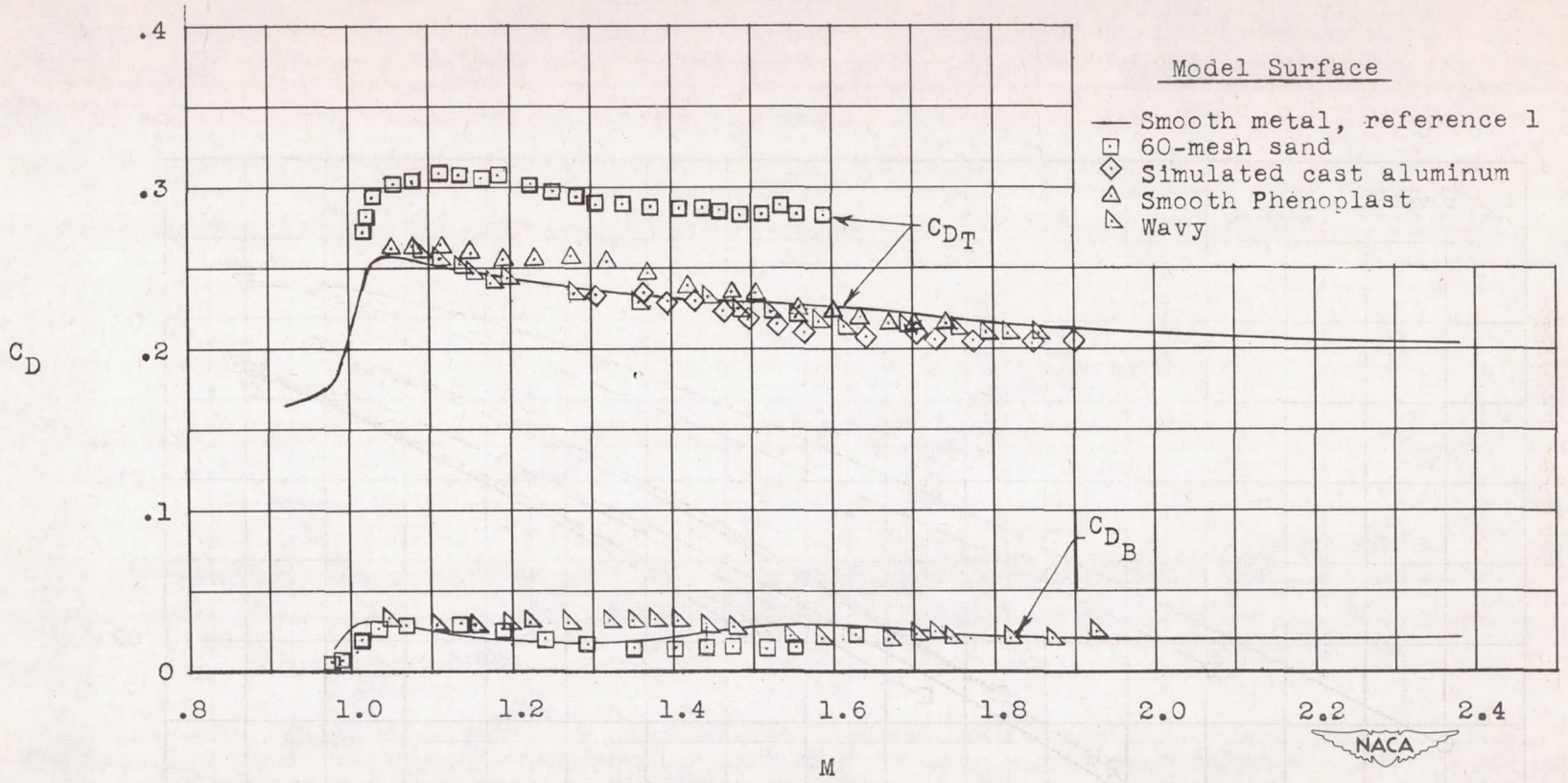


Figure 7.- Variation of total-drag coefficient and base-drag coefficient with Mach number for models of fineness ratio 12.2 having various types of surfaces.

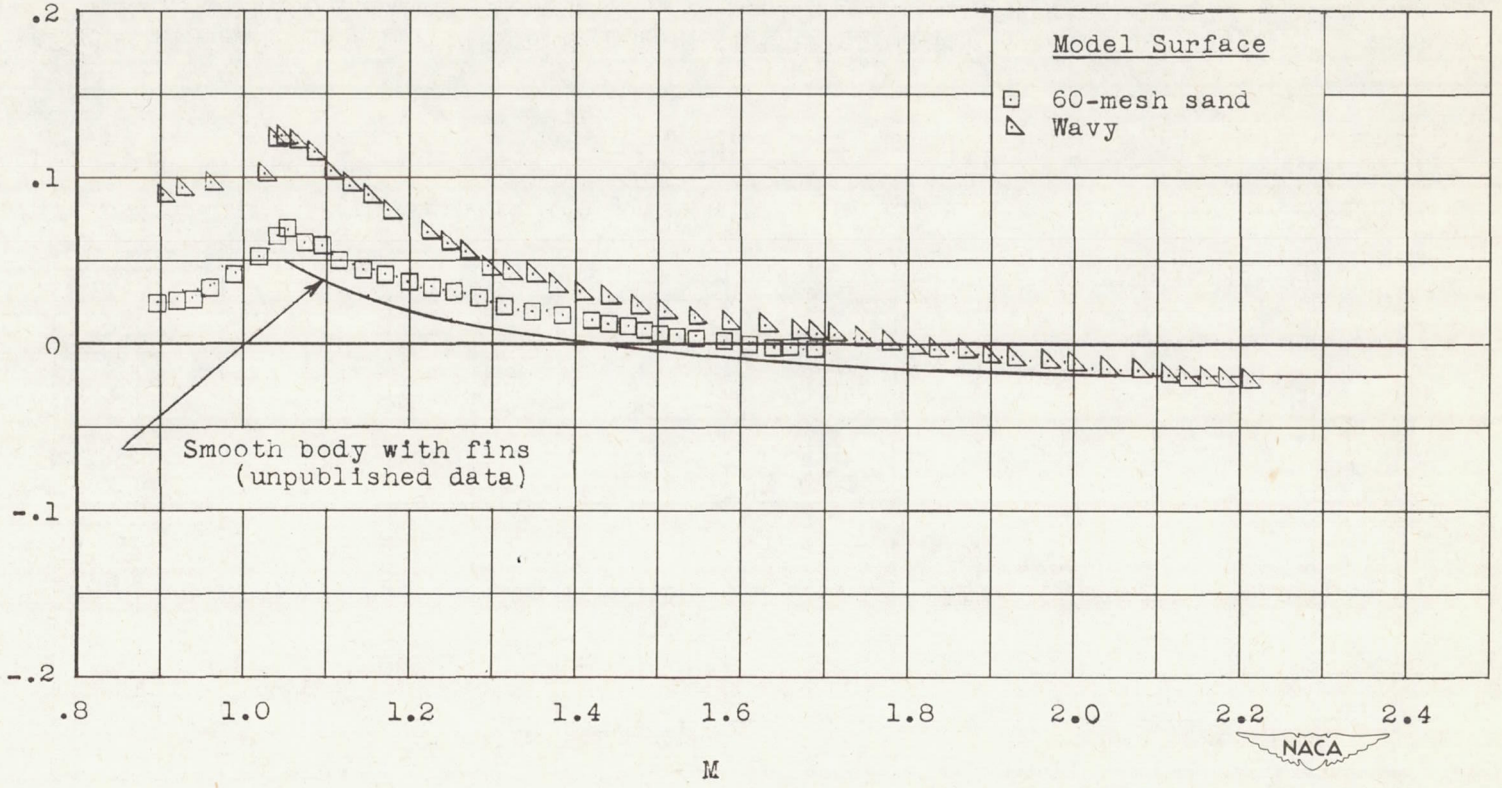


Figure 8.- Variation of pressure coefficient with Mach number for models of fineness ratio 12.2 having various types of surfaces. Pressure measured at $\frac{x}{l} = 0.9075$; 45° between fins.

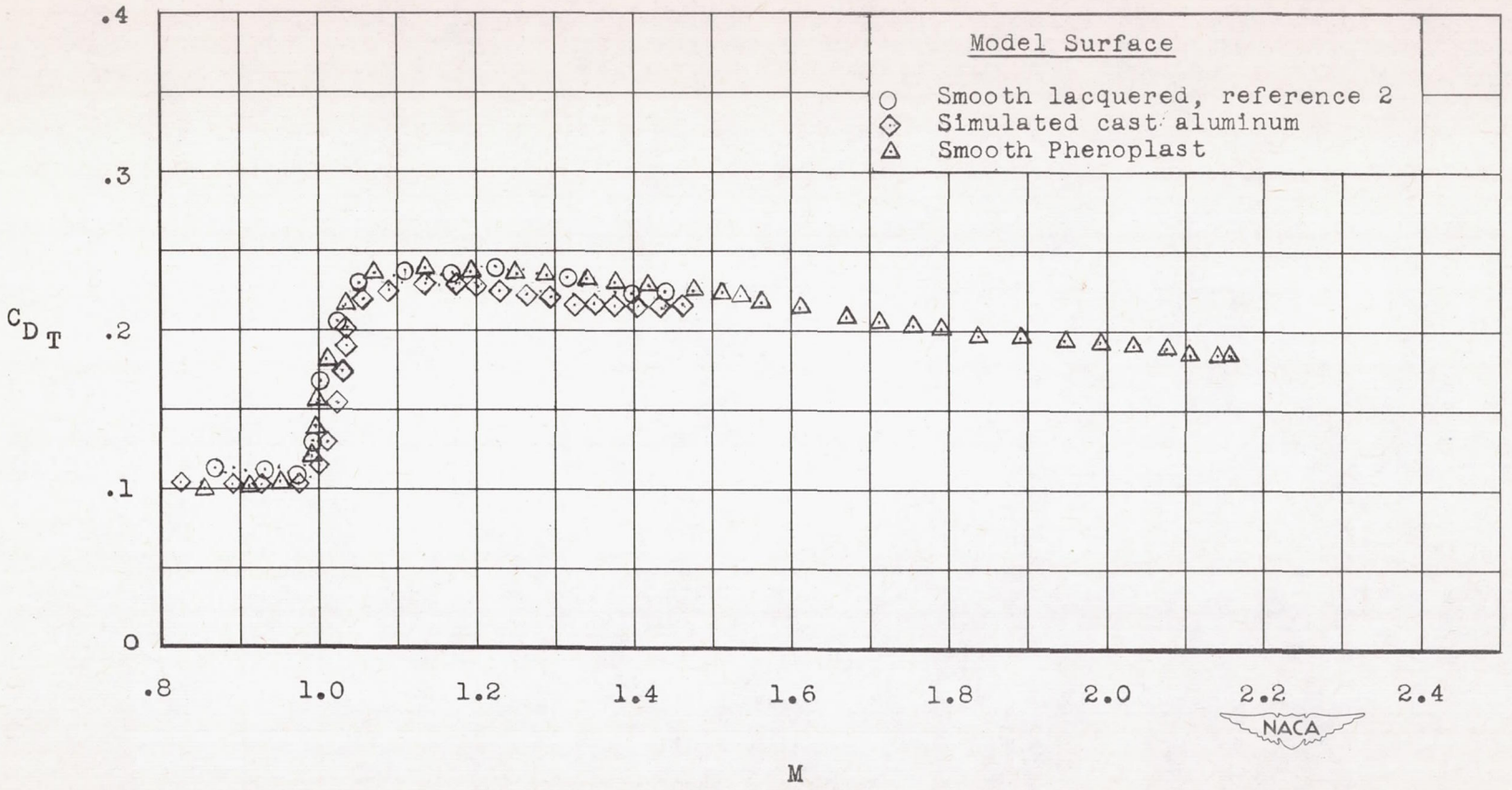


Figure 9.- Variation of total-drag coefficient with Mach number for models of fineness ratio 8.91 having various types of surfaces.

NACA-Langley